The Compass: Earth Science Journal of Sigma Gamma Epsilon

Volume 85 | Issue 1 Article 2

7-30-2013

P-T Constraints of Orthogneiss, Metapelites, and Ultra-Mafic Lenses Located in the Virgin Mountains of Northwestern Arizona

Bryan R. Nielson
Southern Utah University, bassman_119@yahoo.com

Brady M. Nielson
Southern Utah University, nielson_218@yahoo.com

Andrew Schroeder
Southern Utah University, abschroeder13@gmail.com

Mark R. Colberg
Southern Utah University, colberg@suu.edu

P-T CONSTRAINTS OF ORTHOGNEISS, METAPELITES, AND ULTRA-MAFIC LENSES LOCATED IN THE VIRGIN MOUNTAINS OF NORTHWESTERN ARIZONA

Bryan R. Nielson, Brady M. Nielson, Andrew Schroeder, & **Mark R. Colberg**
Department of Physical Science
Southern Utah University
Cedar City, UT 84720, USA
bassman_119@yahoo.com
nielson_218@yahoo.com
andrew.b.schroeder@gmail.com
colberg@suu.edu

ABSTRACT

The Virgin Mountains, located in northwestern Arizona, host a variety of different geologic features. Many workers have focused on Tertiary extension within the mountain range, but little work has been done on the Paleo-Proterozoic basement rocks. Tertiary extension has exposed 1.73 – 1.80 Ga basement material that exhibits intense shear deformation and evidence of high temperature/high pressure and possibly ultra-high pressure metamorphism. These rocks are well exposed throughout Elbow and Lime Kiln Canyons, which are located east and south of Mesquite, Nevada. Some exposures enclose ultra-mafic lenses containing pyroxene/spinel pseudomorphs after garnet. These features suggest decompression through the garnet-spinel transition. These rocks occur in a broad shear zone exposed over 80-100 km in the Virgin Mountains and the Beaver Dam Mountains to the north. Most samples are mylonitic, but contain polygonal quartz grains consistent with shearing under high-temperature conditions. Other shear indicators include sigma and delta structures, mica-fish and S-C textures. Sillimanite and biotite within the S-C shear fabric suggest deformation and equilibration under upper amphibolite to lower granulite facies conditions (650^{o}-800^{o}C and 0.6-1.1 Kilobars). Also, sillimanite pseudomorphs after kyanite found within metapelites suggests decompression from high pressure conditions. Decompression of ultra-mafic lenses through the garnet-spinel transition documents pressures in excess of 2.0 GPa and depths of at least 70 Km. Structural considerations as well as the presence of high-pressure metamorphism are consistent with a collisional suture. The Virgin Mountains appear to host the Paleoproterozoic collisional boundary between Mojave and Yavapai crustal provinces.

KEY WORDS: Virgin Mountains, Elbow Canyon, Lime Kiln Canyon, Beaver Dam Mountains, orthogneiss, metapelites, metamorphism, amphibolites facies, granulite facies, Mojave crustal province, Yavapai crustal province, Laurentia

INTRODUCTION

Ongoing metamorphic studies are providing new data that improve our understanding for the assembly of southwestern Laurentia. Exposures of lower crustal rocks in the Beaver Dam Mountains in southwestern Utah and the Virgin Mountains of northwestern Arizona (Fig. 1) document high pressure/ ultrahigh pressure (HP/ UHP) conditions and partial subduction of the Yavapai province beneath the Mojave province. The Virgin Mountains are characterized by a broad (km-scale width) zone of intense shearing resulting from compressional and transpressional motions (Quigley *et al.*, 2002; Colberg, 2011). The Virgin Mountains correlate with the Beaver Dam Mountains in Utah and should record similar P-T conditions as its northern counterpart. This work reports a first petrological study examining Paleo-Proterozoic orthogneisses, and metapelites and their associated ultra-mafic lenses located in the Virgin Mountains of northwestern Arizona.

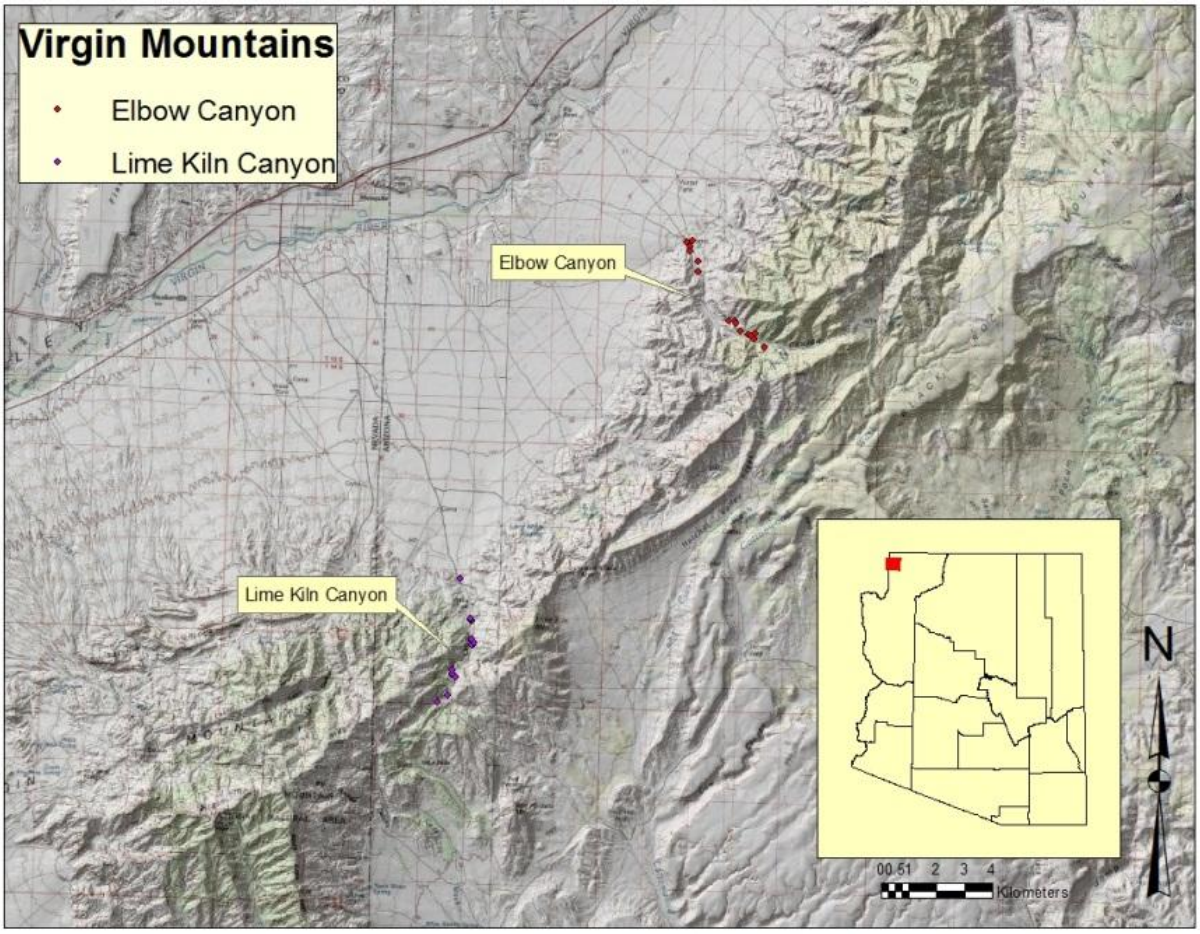

Figure 1. Shaded relief map of the Virgin Mountains, Arizona and Nevada. Dots depict sample locations in Elbow and Lime Kiln Canyons.

GEOLOGIC SETTING

Paleo-Proterozic Yavapai and Mojave crust exposed throughout northwestern Arizona consists of complexly deformed meta-igneous and meta-sedimentary rocks. Extension and isolated uplifts from the Basin and Range province have exposed this material across much of northwestern Arizona, including the Virgin Mountains. The two provinces were originally defined through differences in ages and Pb isotope characteristics (Bennett and DePaolo, 1987). Pb isotopes show that the Yavapai Province developed from a primitive source while the Mojave Province developed from a more evolved source (Bennett and DePaolo, 1987). Nd model ages yield 1.68 – 1.78 Ga for Yavapai crust, and ages in excess of 2.0 Ga for Mojave Province crust. These age characteristics were used by these authors to define a boundary that underlies a portion of the present day Basin and Range Province in Nevada (Fig. 2). Wooden and Mojave Provinces. Duebendorfer *et al*. (2006) suggested a revised boundary trending northwest of the Cherbat DeWitt (1991) defined a northeast trending zone of isotopically mixed Paleo-Proterozic crust spanning a width of 75 km exposed in the Grand Canyon. This zone, which contains rocks originating from both provinces, is often considered the boundary between the Yavapai and Mountains in Arizona on the basis of geophysical evidence (Fig. 2).

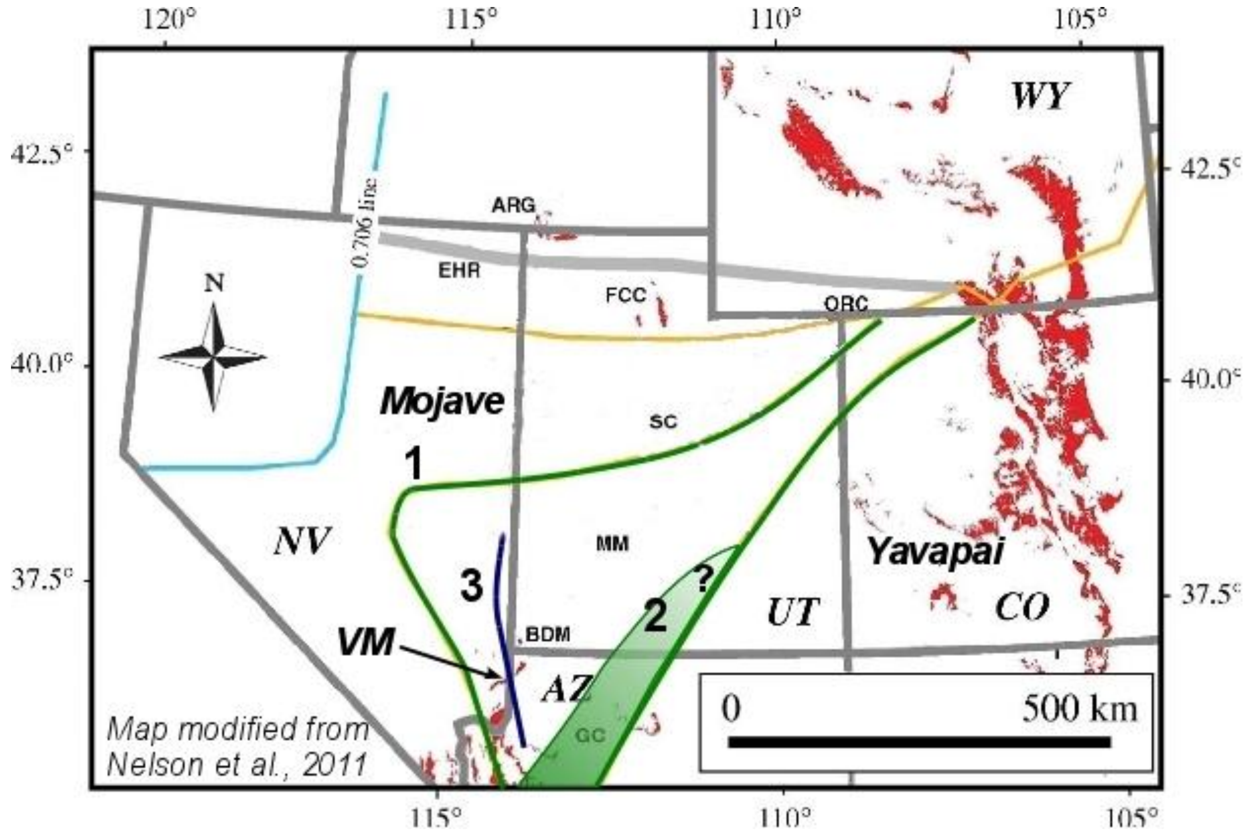

Figure 2. Regional map showing proposed boundaries separating the Mojave Province from the Yavapai Province: **(1)** Original boundary proposed by Bennett and DePaolo (1987); **(2)** eastern edge of isotopically mixed zone originally proposed by Wooden and DiWitt (1991); and **(3)** boundary proposed by Duebendorfer *et* al. (2006) and northern extension proposed in this study. The extended boundary passes through the Virgin Mountains in green. Map modified from Nelson *et al*., 2011.

Rocks from both provinces are exposed in the Virgin Mountains. Low pressure granulite facies rocks from the Mojave Province are exposed on the west side of the mountain range. Amphibolites to high pressure granulite facies rocks, similar to those in the Beaver Dam Mountains (Colberg, 2011; Fitzgerald and

Colberg, 2008) occur on the east side of the Virgin Mountains. These rocks are separated by a nearly 5-km-wide zone of intensely sheared rocks (Fig. 3a and 3b). The eastern side of the shear zone contains large lenses of ultra-mafic material thought to have a mantle origin. These rocks, which lie along the northward extension proposed by Duebendorfer *et* al. (2006), are consistent with formation in a collisional setting.

METHODS

Samples of Paleo-Proterozoic rocks were collected from both Lime Kiln and Elbow Canyons in the Virgin Mountains (Fig. 1). Chemical data from selected samples were collected using the JOEL JXA-8900 electron microprobe at the University of Nevada Las Vegas. For orthogneiss assemblages, P-T conditions were estimated using the Holland and Blundy (1994) amphibole-plagioclase thermo-meters. For metapelitic rocks, temperatures were estimated using the garnet-biotite (Williams and Grambling, 1990), garnet-phengite (Green and Helman, 1982) and Ti-in-biotite (Henry, et al., 2005) geothermometers. Koziol and Newton's (1988) geobarometer for pelitic assemblages, Green and Hellman's (1982) geothermometer and Koziol and Newton's (1988) geobarometer were correspondingly used to estimate P-T conditions using garnet and phengite assemblages. These calibrations were then plotted on the open source Veusz scientific plotting program to illustrate the P-T results.

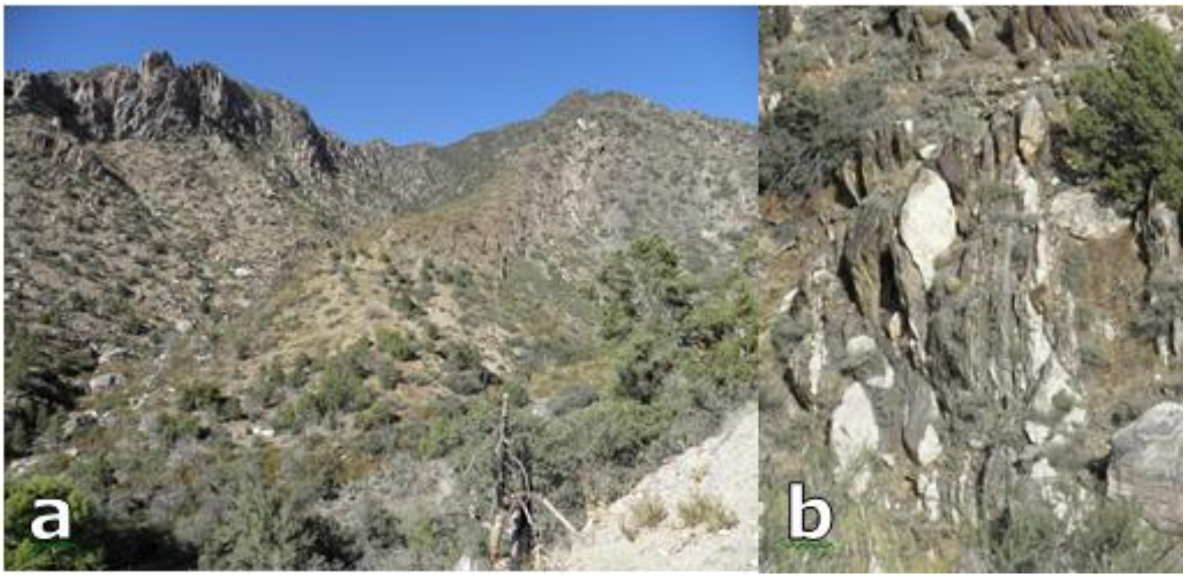

Figure 3. Intensely deformed rocks from the broad shear zone within the Virgin Mountains. **a)** View of cliff face and slope on north side of Elbow Canyon. Note well defined, near vertical shear foliation. Width of view approximately 0.5 Km. **b)** Large, metagranitoid boudins contained in intensely deformed orthogneiss, Lime Kiln Canyon, Boudins are approximately 2-3 meters in length.

MINERAL CHEMISTRY RESULTS

Orthogneiss

Orthogneiss assemblages evaluated in this study consist of quartz + plagioclase + amphibole + biotite (Fig. 4a). These samples are mylonitic and were collected from the sheared portion of Lime Kiln and Elbow Canyons. Quartz frequently displays undulatory extinction, sub-grain development, and serrated-sutured grain boundaries (Fig. 4b). However, quartz may also be observed as a granoblastic polygonal texture in some parts of the orthogneiss. Most plagioclase occurs as hybidioblastic to xenoblastic and display moderately to poorly preserved crystal faces. In many cases, plagioclase is perthitic and reveals undulose extinction. Twinning in plagioclase has been altered and is displayed as deformation twins concentrated in areas that have undergone higher intra-crystalline deformation. Inclusions within the plagioclase include quartz, biotite, and other minerals. Amphibole occurs as irregular xenoblastic grains with poor crystal face development. In certain cases, amphibole assumes a sigmoidal shape resulting from the pervasive shearing characteristic (Fig. 4b and 4c). Amphibole may contain inclusions of biotite, quartz, plagioclase and other phases. Biotite occurs as both sub-euhedral grains and fibrous aggregates that parallel the foliation, and occasional mica-fish. The orthogneiss displays foliation reflecting s-c fabric (fig. 4c) which resulted from shear (Passchier and Trouw, 2005).

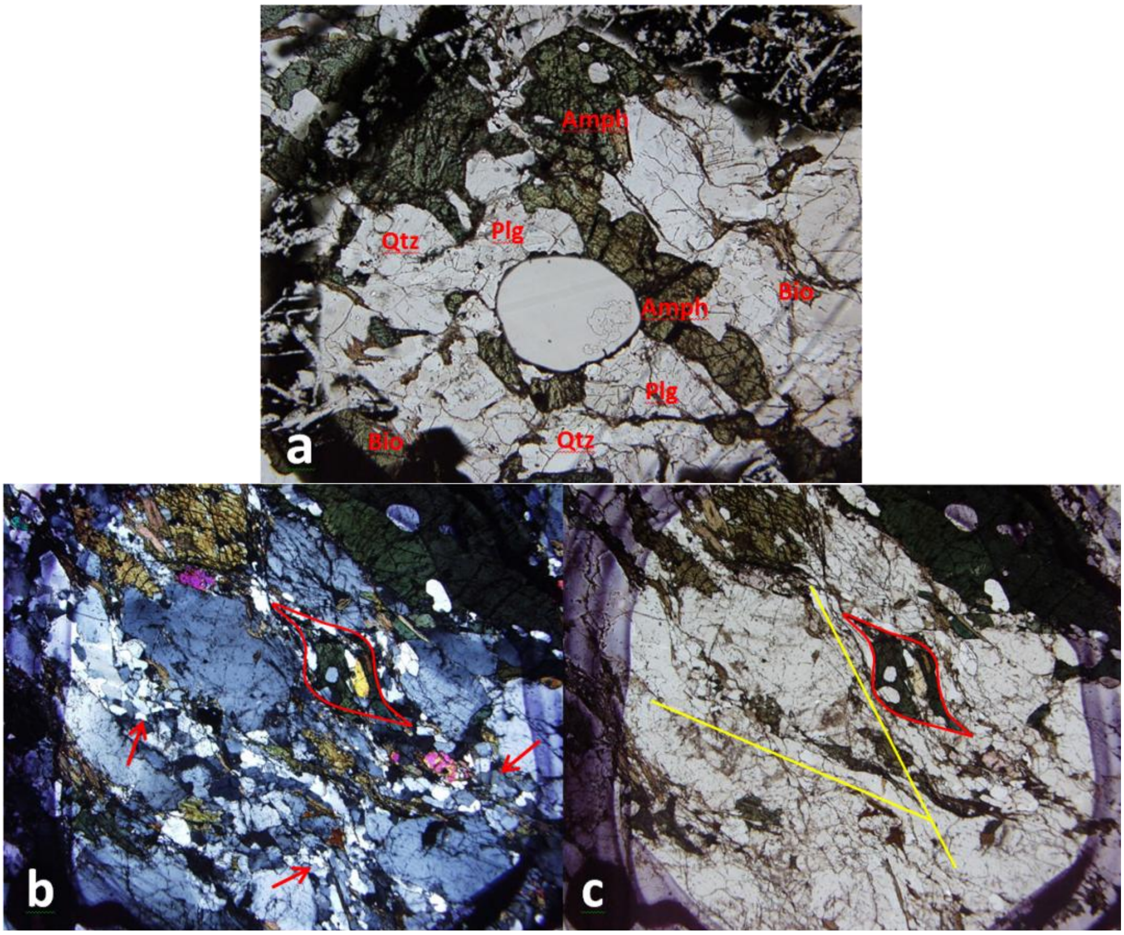

Figure 4. Photomicrographs of the orthogneiss, **(a)** Common mineral assemblage consisting of quartz (Qtz), plagioclase (Plg), amphibole (Amph), and biotite (Bio). Plane polarized light. **(b)** Sheared orthogneiss. Sigmoidal amphibole and plagioclase define well developed c-s fabric (yellow lines). Note polygonal quartz suggesting high temperature deformation. Crossed polarized light. **(c)** Same and **(b).** Plane polarized light.

Two samples of orthogneiss were selected for analysis with the electron microprobe, one from Elbow Canyon (VMEC 11-2), and one from Lime Kiln Canyon (VMLK 11-22). In sample VMEC 11-2, plagioclase compositions range from 59%-64% albite and 35%-38% anorthite. Zonation throughout these grains is low, with an average rim to core variation of ± 1.5% (see Table 3, Appendix 1). Both alkali feldspar and plagioclase were analyzed from sample VMLK 11-22 (Table 7, Appendix 1). Alkali feldspar was found to contain 6%-10% albite, comparatively no anorthite, and 89% - 93% potassium feldspar. There is little zonation in the alkali feldspar with approximately ±2% albite rim to core variation. Plagioclase contains 65%-68% albite, 30%-33% anorthite, and 1.2% potassium feldspar. The plagioclase also shows slight zonation with a ± 3% albite rim to core variation.

Amphibole data were also obtained from samples VMEC 11-2 and VMLK 11-22 (Table 4 and Table 8 in appendix 1). The majority of amphiboles in VMEC 11-2 are pargasite, although tschermakite and magnesiohornblende are also present. Amphiboles in sample VMLK 11-22 have a slightly higher $^{[A]}$(Na + K) sum than the amphiboles in sample VMEC 11-2, and are also classified as pargasite. Amphibole compositional data from both samples (VMEC 11-2 and VMLK 11-22) are plotted in Figure 5. Amphibole nomenclature follows Leake *et al*., (1997).

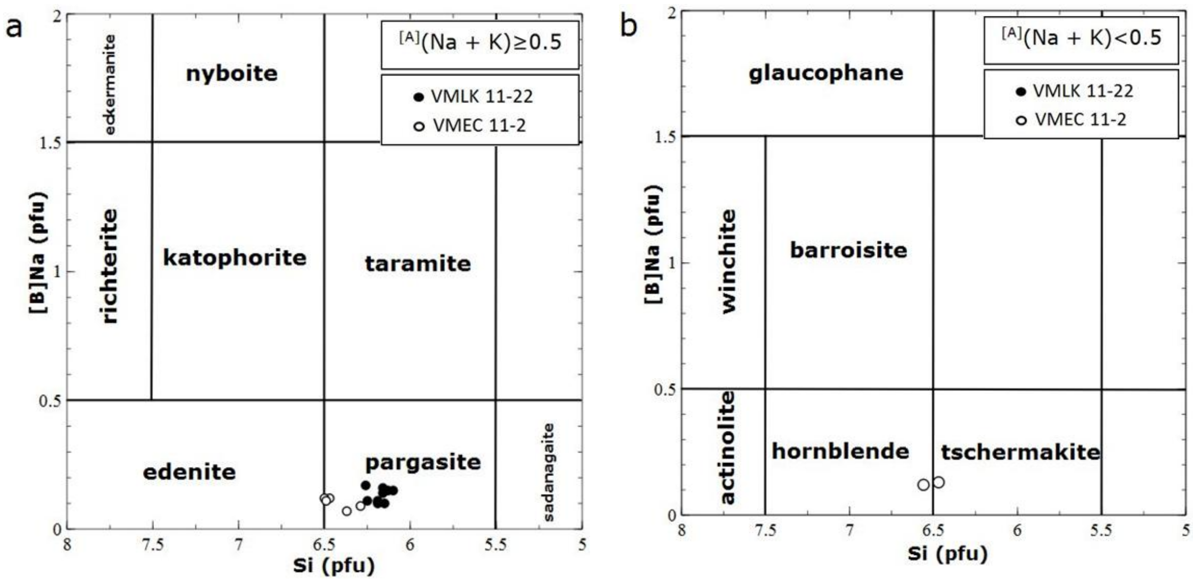

Figure 5. Compositions of amphibole from orthogneiss. Filled circles – Lime Kiln Canyon. Unfilled circles – Elbow Canyon. Most amphiboles are classified as pargasite. After Leake *et* al., 1997.

Metapelites

Although less abundant than the orthogneiss, metapelites are an important constituent of the sheared rocks exposed in the Virgin Mountains. Metapelites occur as layers intercalated with the orthogneiss in both Elbow and Lime Kiln Canyons. However, major differences occur between rocks collected from either canyon.

Metapelites sampled from Elbow Canyon consist of quartz + garnet + biotite + muscovite + sillimanite + plagioclase

(Fig. 6a). Subordinate amounts of rutile and ilmenite are also present. Most of these rocks are strongly mylonitic, reflecting intense shearing. Quartz commonly displays sub-grain development, serrated grain boundaries, and often appears as elongate ribbons. Garnets are xenoblastic with poorly developed crystal faces and occasionally occur as strongly deformed sigmoidal grains (Fig. 6a and 6c). Most garnet contains isolated inclusions of rounded biotite, quartz, and plagioclase (Fig. 6b). In the body of the rock, biotite, muscovite and sillimanite occur in a number of textural relationships, and document different parts of the metamorphic and deformational history. Pre-kinematic biotite occurs as relict grains and "fish" truncated by the primary mylonitic foliation. This early biotite and garnet both predate shearing and could be contemporaneous. Fine-grained aggregates of biotite, muscovite, and sillimanite parallel the stretching direction of quartz and partially define the primary mylonitic foliation. Muscovite appears to be one of the last phases to crystallize as it occurs as an overgrowth on biotite. Intergrowths of biotite and sillimanite may reflect the breakdown of an early generation of garnet. Sillimanite also occurs as centimeter-scale bladed aggregates interpreted as pseudomorphs after kyanite (Fig. 6e). On very rare occasions, relict kyanite can be observed (Fig. 6f).

Plagioclase occurs primarily as pre-kinematic, rounded and lensoidal grains elongated parallel to the shear foliation. Plagioclase frequently displays wedge-shaped, non-penetrating deformation twin lamella. Alkali feldspar was observed only in metapelites sampled in Lime Kiln Canyon. These occur as antiperthitic feldspars and mesoperthites (Fig. 6d) which probably represent exsolved ternary feldspars. Perthites occur as rounded grains in lenses which are thought to represent pre-kinematic leucosome.

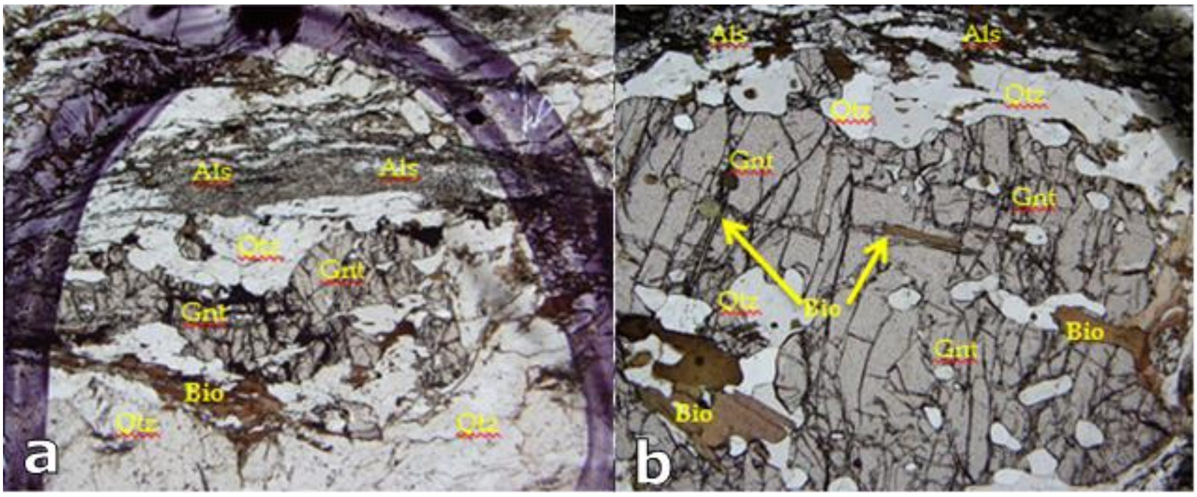

Figure 6. Mineralogy and textural features characteristic of metapelite from Elbow and Lime Kiln Canyons. (a) Deformed metapelite from Lime Kiln Canyon (VMLK 20-23) containing quartz (Qtz), plagioclase (Plg), biotite (Bio), Alluminosilicate (sillimanite (Als)), and garnet (Gnt). Note sigmoidal shape of garnet. Plane polarized light.

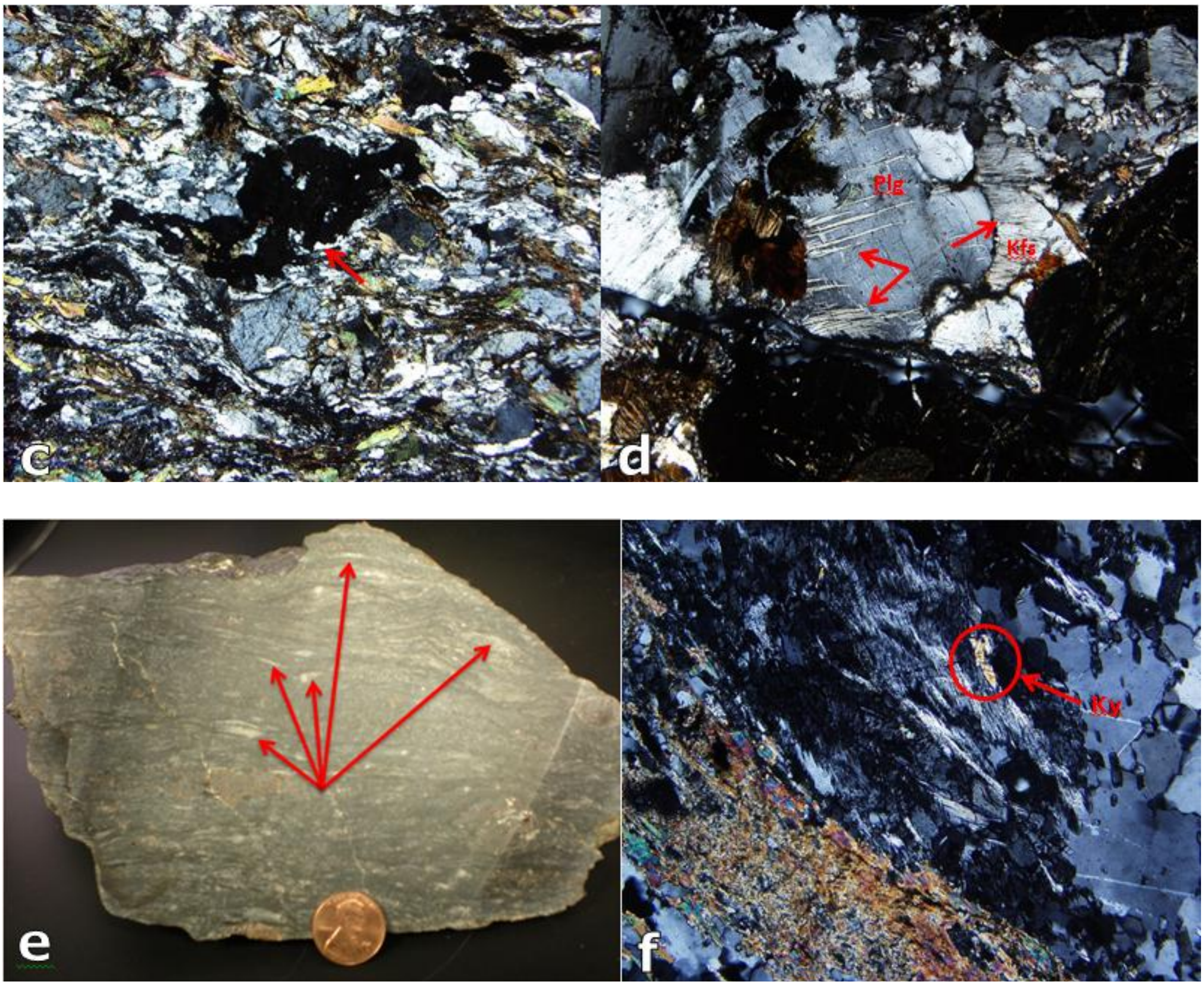

Figure 7 (continued). Mineralogy and textural features characteristic of metapelite from Elbow and Lime Kiln Canyons. **(b)** Garnet porphyroblast contained in schist from Elbow Canyon (VMEC 11-14). Note rounded inclusions of biotite (Bio). Plane polarized light. **(c)** Sigmoidal garnet in strongly mylonitized matrix. Crossed polars. **(d)** Perthitic K-feldspar (Kfs) and plagioclase (Plg) from leucosome in metapelite from Elbow Canyon (VMEC 11-14). **(e)** Bladed aggregates of sillimanite thought to be pseudomorphs after kyanite. **(f)** Photomicrograph showing relic kyanite (circle) within sillimanite.

Microprobe analyses were performed on samples from Elbow Canyon (VMEC 11-14) and Lime Kiln Canyon (VMLK 20-23). Garnet compositions from sample VMEC 11-14 (Table 2 in Appendix 1) show little variation and average 75% almandine, 18% pyrope, 2.7% grossular, and 2.9% spessartine. Compositions from the core and rim are generally similar. Garnets from VMLK 20-23 are iron rich and contain 53% - 56% almandine, 3% - 4% grossular, 9% - 11% pyrope, and are unusually rich in spessartine (29% - 33%).

Garnets from the Elbow Canyon sample (VMEC 11-14) contain abundant rounded biotite inclusions. The inclusions are relatively aluminous (Table 1) and contain 0.133 to 0.342 apfu titanium. Mg/(Mg+Fe) ranges from 0.573 to 0.635. Matrix biotite from VMLK 20-23 contains 0.287 to 0.429 apfu titanium. Mg/(Mg+Fe) ranges from 0.555 to 0.592.

Compositional data were also collected for select muscovite grains in sample VMLK 20-23 (table 9 in appendix 1). Muscovite is slightly phengitic with Si ranging from 6.15 to 6.20 apfu calculated on 24-oxygen basis. Mg ranges from 0.15 to 0.19 apfu and Fe ranges from 0.30 to 0.34 apfu.

Plagioclase in sample VMEC 11-14 contains 33%-40% anorthite, while plagioclase from sample VMLK 20-23 contains 32%-37% anorthite. Plagioclase compositions were estimated using optical methods.

Ultramafics

Lenses of ultramafic rocks located on the eastern edge of the shear zone comprise of amphibole + olivine + clinopyroxene + orthopyroxene + spinel. These lenses are enclosed within sheared metagranitoids and paragneiss, and are elongated parallel to foliation of the country rock. The interiors of the ultra-mafic lenses are relatively undeformed. The edges of the lenses contain retrograde phlogopite and are more intensely deformed than the interiors. The more pristine ultra-mafic rock contains round aggregates of orthopyroxene and spinel with subordinate clinopyroxene (Fig. 7a). These aggregates are contained in a granoblastic matrix consisting of pargasitic amphibole and orthopyroxene porphyroclasts (Colberg, 2011). The orthopyroxene contains abundant exsolution lemella of spinel, illmenite, garnet, and clinopyroxene (Fig. 7a and 7b; Colberg, 2011). The pyroxene-spinel aggregates are thought to indicate the former presence of garnet and decompression of the ultramafic rock through the garnet spinel transition. Exsolution lamella within the orthopyroxene is consistent with growth under ultra-high pressure conditions (Zhang and Liou, 1999; Colberg, 2011).

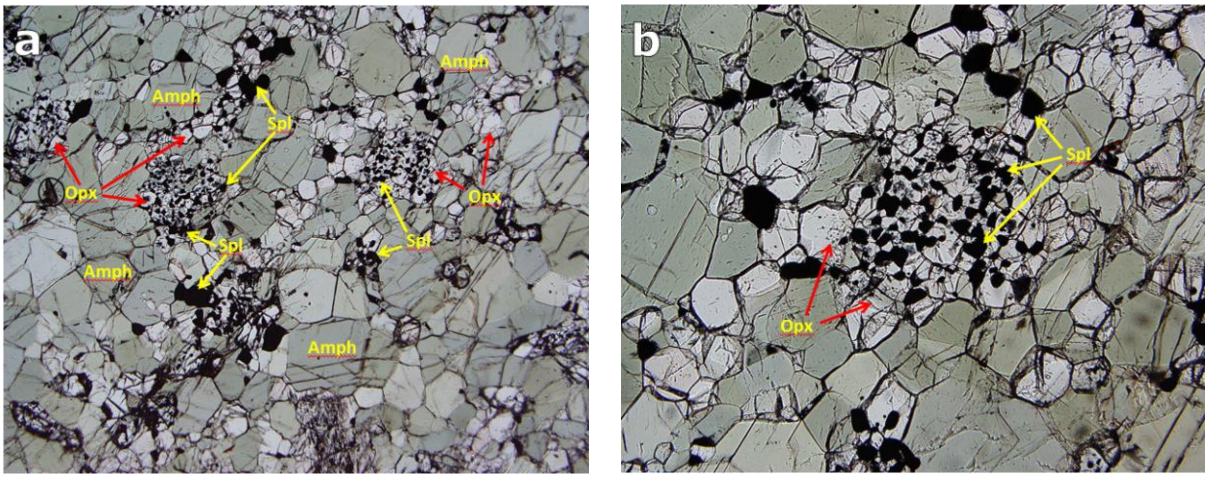

Figure 8. Mineralogy and textural features in ultra-mafic rock from Lime Kiln Canyon. **(a)** Round fine-grained aggregates of orthopyroxene (Opx, red arrows) and spinel (Spl, yellow arrows) in a granoblastic matrix consisting of pargasitic amphibole and spinel. **(b)** Round orthopyroxene-spinel aggregate.

Geothermobarometry

A number of geothermobarometers are available for estimating the pressure-temperature (P-T) conditions of metamorphism. Both metapelites and orthogneiss were examined during this study, and both present unique challenges when estimated P-T conditions.

Geothermobarometers are best developed for metapelitic rocks and utilize biotite, phengite, and garnet compositions. The orthogneisses in this study contain hornblende and plagioclase, so geothermobarometers developed for the more mafic amphibolites were used for these rocks.

Metapelites

Three independent techniques were used for estimating temperatures within the metapelites: titanium in biotite geothermometer (Henry *et al*., 2005), garnet-biotite geothermometer (Williams and Grambling, 1990), and garnet-phengite geothermometer (Green and Hellman, 1982). All of these geothermometers yielded very similar results for matrix assemblages. Because the titanium in biotite geothermometer (Henry *et al*., 2005) depends only on biotite compositions, temperatures could be estimated for biotite inclusions in garnet. Titanium in biotite geothermometer yielded temperatures of 670–731°C for biotite in the matrix (Table 1). The garnet-phengite geothermometer yielded temperatures between 770-820°C and the garnet-biotite geothermometer yielded temperatures of 625-675°C (Fig 8a, and 8b; Table 1). Both thermometers used biotite in the matrix.

Equilibrium between garnet, sillimanite, plagioclase, and quartz (GASP, Koziol and Newton, 1998; Spear, 1993) were used to estimate pressures. This geobarometer was solved using a variety of temperatures. The intersections between the resulting curves for GASP, and the garnet-biotite and garnet-phengite curves, was used to estimate unique P-T conditions (Fig. 8a and 8b). Intersections between the curves yielded temperatures in the range of 625-820°C and pressures between 0.5-0.8 GPa. When compared to titanium-in-biotite, temperature inter-sections with GASP yield pressures between 0.4 and 0.55 GPa. All of these P-T estimates are within error assuming ±50°C and ±0.2 GPa errors.

The titanium-in-biotite geothermo-meter yielded temperatures in the range of 502-565°C when applied to biotite inclusions within garnet from Elbow Canyon samples (Table 1). A second group of temperatures for inclusions within a separate garnet yielded 683-703°C temperatures, which are consistent with conditions determined for matrix assemblages. Pressures could not be determined since plagioclase could not be observed as inclusions within the garnets.

Sample	Ti	Mg/(Mg+Fe)	T(°C)
11-22 C2B1	0.429	0.461	713
11-22 C2B2	0.426	0.467	713
11-22 C2 B2P1	0.354	0.432	680
11-22 C4 B1P1	0.42	0.441	707
11-22 C4 B2P1	0.341	0.451	677
20-23 C2 B1P1	0.432	0.557	731
20-23 C2 B1P2	0.394	0.574	723
20-23 C3 B1P1	0.287	0.592	681
20-23 C4 B1P1	0.289	0.547	670
20-23 C4 B1P2	0.301	0.541	675

Sample	Ti	Mg/(Mg+Fe)	T (°C)
VMEC14-C1B1	0.342	0.573	703
VMEC14-C1B2	0.277	0.494	651
VMEC14-C1B3	0.288	0.595	683
VMEC14-C2B1	0.137	0.635	560
VMEC14-C2B2	0.148	0.608	565
VMEC14-C2B3	0.151	0.589	561
VMEC14-C2B4	0.133	0.522	502

Figure 9. Plots of equilibria used to constrain temperatures and pressures of the metapelites. Intersections are used to estimate P-T conditions. **(a)** Intersections of the garnet-phengite Fe-Mg exchange thermometer with the GASP barometer. Sample VMLK 20-23 from Lime Kiln Canyon. **(b)** Intersections of the garnet-biotite thermometer with the GASP barometer for sample VMEC 11-14 from Elbow Canyon.

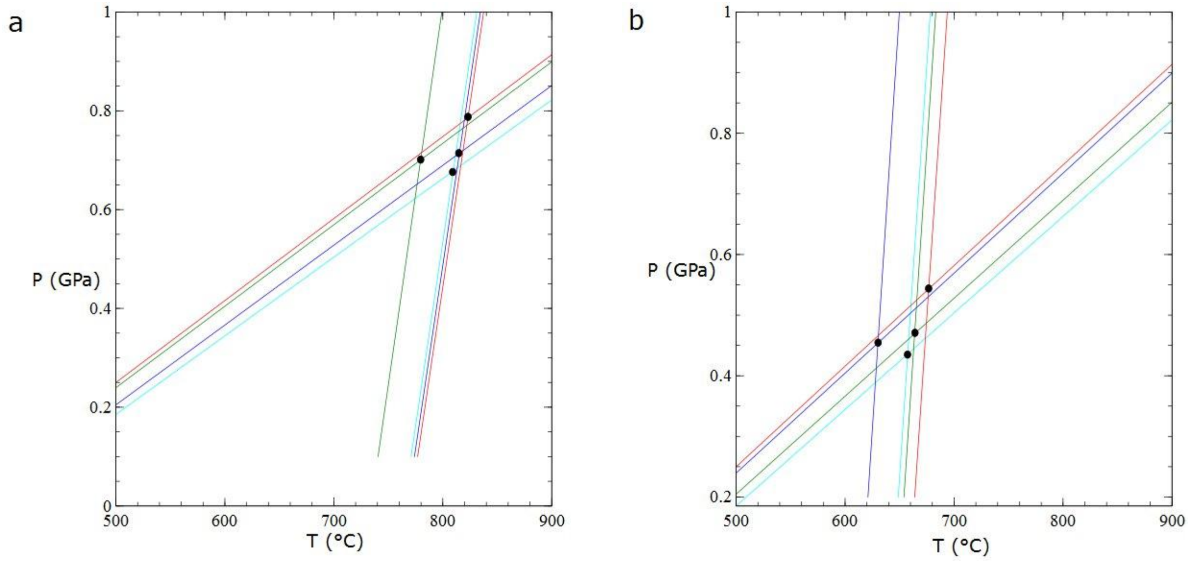

Figure 10. Plots of equilibria used to constrain temperatures and pressures of the metapelites. Intersections are used to estimate P-T conditions. **(a)** Intersections of the garnet-phengite Fe-Mg exchange thermometer with the GASP barometer. Sample VMLK 20-23 from Lime Kiln Canyon. **(b)** Intersections of the garnet-biotite thermometer with the GASP barometer for sample VMEC 11-14 from Elbow Canyon.

Orthogneiss:

P-T conditions for the hornblende bearing orthogneiss were estimated using the hornblende plagioclase geothermometers of Holland and Blundy (1994) and the Ti-Al-in-amphibole geothermo-barometry of Ernst and Liu (1998). The Holland and Blundy (1994) geothermometers rely on two reactions involving plagioclase and hornblende. The Holland and Blundy (1994) geo-thermometer yielded temperatures in the range of 680-740°C for sample VMEC 11-2 in Elbow Canyon, and 730-760°C for VMLK 11-22 in Lime Kiln Canyon (Fig. 9a and 9b). Holland and Blundy (1994) report maximum ±40°C errors for these geothermometers. The two reactions have steep positive and negative slopes that generally intersect at a low angle. This imparts large errors if the two reactions are used for pressure determinations.

The empirical geothermometer of Ernst and Liu (1998) relies on titanium and aluminum concentrations in hornblende that vary systematically with pressure and temperature. This provides an independent pressure estimate for amphibole bearing rocks. When TiO_2 and Al_2O_3 data are plotted, sample VMEC 11-2 yields temperatures in the range of 625-700°C and pressures ranging from 1.0-1.5 GPa. Sample VMLK 11-22 yields temperatures in the range of 775-825°C and pressures ranging from 1.1-1.8 GPa (Fig. 9c).

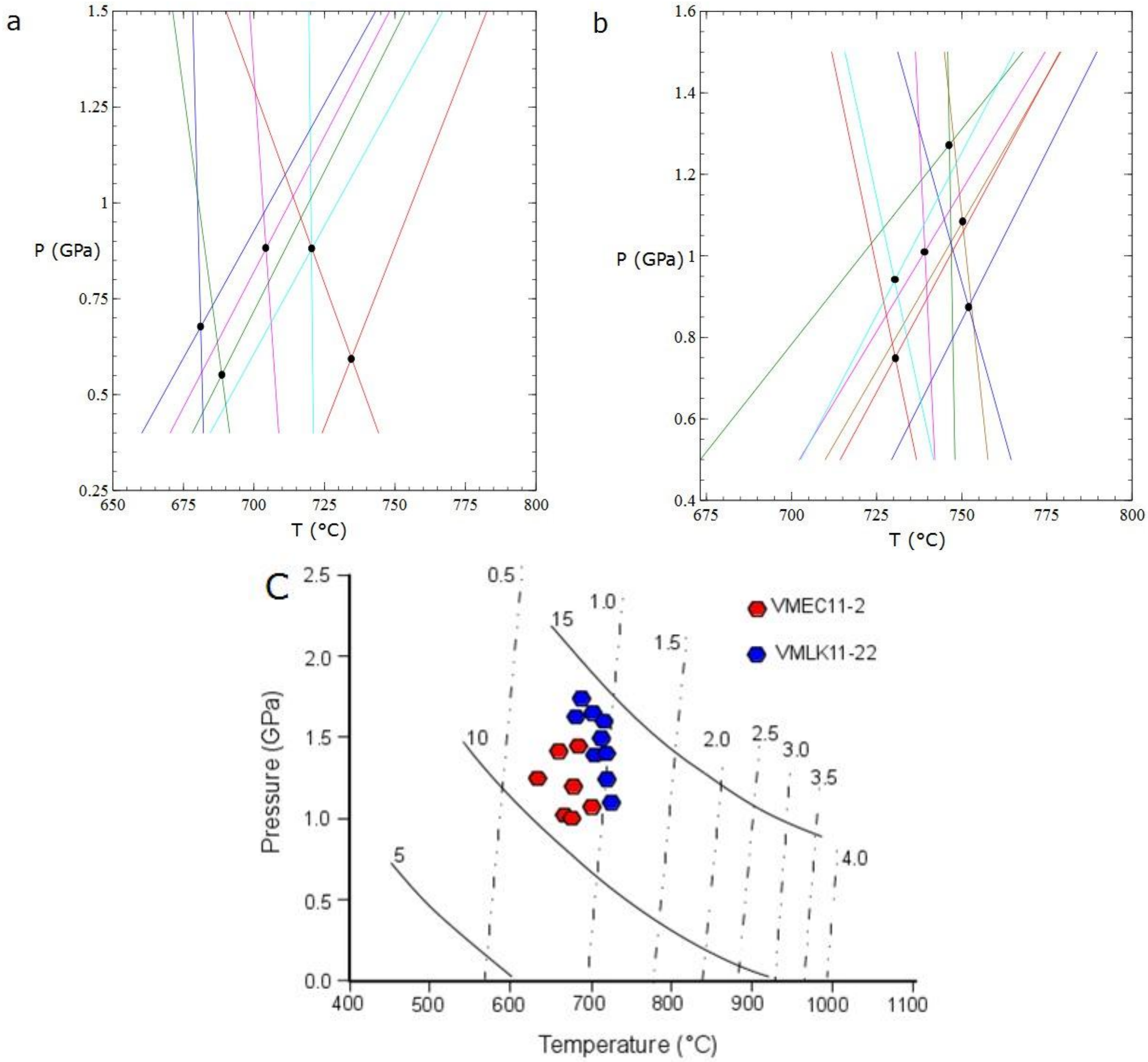

Figure 11. P-T estimates for orthogneiss. **(a)** Plots of equilibria calculated with the hornblende-plagioclase thermometer (Holland and Blundy, 1994) for orthogneiss from Elbow Canyon (VMEC 11-2). **(b)** Plots of eqiilibria calculated with the hornblende-plagioclase thermometer (Holland and Blundy, 1994) for orthogneiss from Lime Kiln Canyon Canyon (VMLK 11-22). **(c)** P-T estimates for VMEC 11-2 and VMLK 11-22 using amphibole compositions after (Ernst and Liu, 1998).

DISCUSSION:

The Virgin Mountains and Beaver Dam Mountains constitute a continuous arcuate mountain range. Tertiary extension exposed underlying 1.73-1.8 Ga Paleo-Proterozic basement rocks. The basement rocks in the Virgin Mountains include a nearly 5-km-wide zone of intensely sheared rocks. This broad shear zone constitutes a structural boundary between rocks of the Mojave Province from rocks of the Yavapai Province (Colberg, 2011). The samples discussed in this paper are representative of rocks from within the shear zone that record the history of collision of these two provinces. The intense shearing and ultra-mafic lenses encountered in the Virgin Mountains are characteristic of collisional sutures.

P-T Path:

The orthogneiss and metapelite from Elbow and Lime Kiln Canyons preserve elements of a clockwise P-T path recording collision, partial subduction and exhumation. Syn-to post-kinematic minerals can be used to constrain post kinematic pressure and temperature conditions. Retrograde biotite in the metapelite as well as apparent replacement of garnet by sillimanite and plagioclase suggest back reaction through the biotite dehydration melting reactions (reaction A, Fig. 10). The lack of retrograde muscovite (reaction B, Fig. 10) and cordierite (reaction C, Fig. 10) constrain pressures and temperatures between 600-750°C and 0.5 and 1.0 GPa (shaded area Fig. 10). Titanium-in-biotite temperatures for syn-to post-kinematic biotite in the matrix constrains temperatures between 670-730°C, which are consistent with estimates based on mineral assemblages (point 1, Fig. 10). Garnet-biotite temperatures and the GASP geobarometer yield averaged temperatures near 650°C and pressure averaging 0.5 GPa (point 2, Fig. 10). Pre-kinematic muscovite fish and garnet can be used to constrain pre-kinematic pressure conditions assuming the two minerals were in equilibrium prior to shearing. Garnet-phengite temperatures ranging between 780-830°C are thought to constrain pre-kinematic temperatures above 1.8 GPa defined by the muscovite melting reaction at these temperatures (point 3, Fig. 10).

Hornblende-plagioclase temperatures range from 675-730°C and 725-750°C for orthogneisses from Elbow Canyon and Lime Kiln Canyon, respectively. P-T conditions estimated from amphibole compositions (Ernst and Liu, 1998) range from 625-700°C and F.0-1.5 GPa for Elbow Canyon (point 4, Fig. 10) and 680-730°C and 1.F-1.8 GPa for Lime Kiln Canyon (point 5, fig. 10). These are consistent with temperatures determined using the hornblende plagioclase thermometer and the high pressure conditions for metapelite from Elbow Canyon.

The ultramafic lenses encountered on the east side of the shear zone in Lime Kiln Canyon also provide constraints for high pressure conditions. Here, fine grained aggregates of orthopyroxene and spinel are interpreted as pseudomorphs after garnet. This suggests decompression of these rocks through the garnet spinel transition at pressures between 1.8-2.0 GPa and temperatures between 800-1000°C (point 6, Fig. 10: Poli and Schmidt, 2003). These conditions are consistent with high temperature high pressure conditions determined by other means.

An early period of metamorphism at lower temperatures is indicated by titanium-in-biotite temperatures of 500-565°C for biotite inclusions in garnet. This places temperature constraints on the prograde portion of a clockwise P-T path as shown by point 7 in Figure 10. No pressure constraints are known for the prograde portion of the P-T path, so placement of point 7 in terms of pressure is speculative. This P-T path documents rapid burial (partial subduction) of relatively hot rocks to pressures of at least 2.0-2.5 GPa followed by decompression (exhumation) through the garnet-spinel transition and kyanite-sillimanite transition to amphibolite facies conditions recorded by syn-to-post kinematic mineral assemblages.

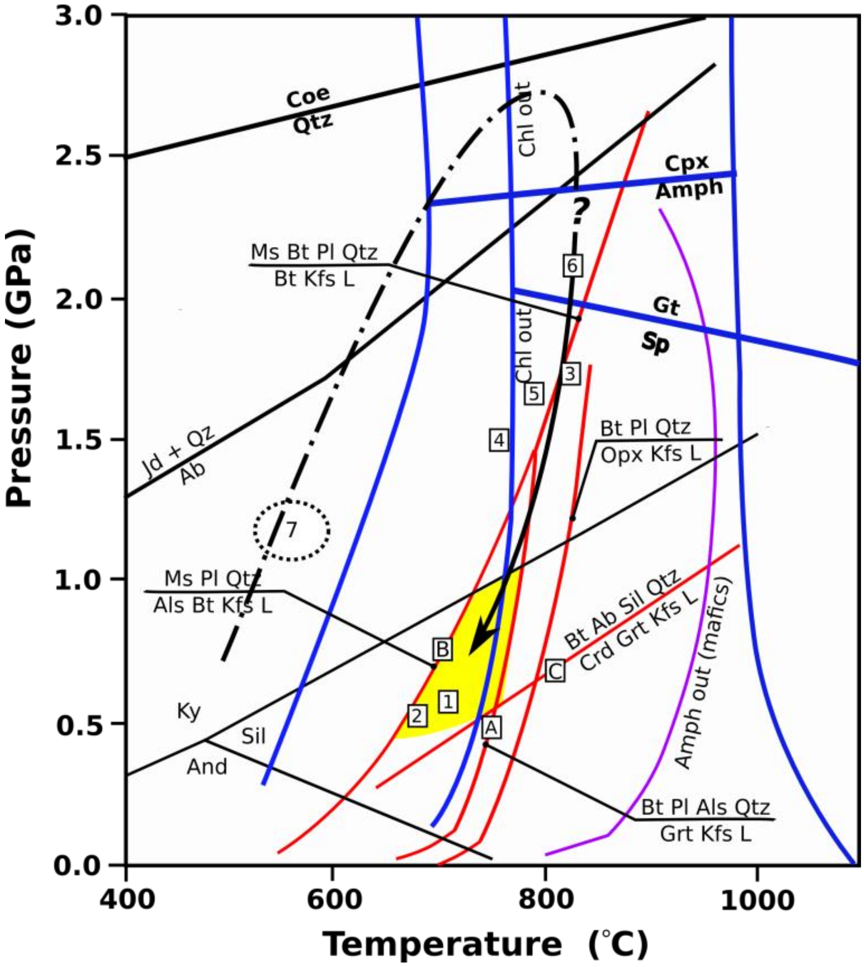

Figure 12. P-T diagram showing bounding reactions and P-T path for rocks in the Virgin Mountains. Red – reactions constraining metapelites. Blue – reactions constraining ultramafic rocks. Mineral assemblages in the metapelites constrain P-T conditions within the yellow shaded area.

Implications

The nature and location of the boundary separating the Yavapai and Mojave Provinces have been debated for many years. Most proposed boundaries have been based on the interpretation of different isotopic characteristics of rocks in various localities. Proposed boundaries include the distribution of Mojave and Yavapai province rocks based on neodymium model ages (Bennett and DePaolo, 1987), which lie to the west of the Virgin Mountains. A zone characterized by mixed lead isotope signatures situated east of the Virgin Mountains (Wooden and DeWitt, 1991) has been accepted by many authors as the boundary between the two provinces. Neither of these boundaries reflects a true structural boundary between the two provinces. The intensely sheared rocks, lenses of ultra-mafic rocks, and evidence for high pressure metamorphism in the Virgin Mountains are consistent with collision and suturing of two fragments of continental crust. This area exposes a structural and metamorphic boundary that separates the two provinces and lies along the northward extension of a structural boundary proposed by Duebendorfer *et al*. (2006). These authors proposed the structural boundary on the basis of geophysical evidence. Evidence presented in this paper and Duebendorfer *et al*. (2006) defines a true tectonic boundary within the Virgin Mountains.

CONCLUSION:

The Paleo-Proterozoic rocks exposed in the Virgin Mountains preserve evidence for high pressure and high temperature metamorphism. These rocks experienced pressures in excess of at least 2.0 GPa. Ultra-mafic rocks containing pyroxene-spinel aggregates of former garnet record decompression through the garnet-spinel transition zone. Pre-kinematic mineral assemblages in the pelitic rocks and amphibole in the orthogneiss record temperatures up to 1.8 GPa. Relic kyanite preserved in pelitic rocks document decompression through the kyanite-sillimanite transition to post kinematic amphibolite facies conditions. These features, together with lower temperature (500-565°C) recorded by biotite inclusions in garnet, document a clockwise P-T path consistent with subduction of continental material in excess of 70 km followed by exhumation to depths of approximately 40 km or less.

The P-T path recorded by these rocks is consistent with subduction and exhumation of continental crust. These metamorphic conditions and fragments of ultra-mafic mantle material situated within a broad zone of intense shearing document collision and suturing of the Mojave and Yavapai Provinces. The rocks exposed in the Virgin Mountains define the true structural and metamorphic boundary separating the Mojave and Yavapai Provinces.

AKNOWLEDGMENTS:

We would like to thank the Undergraduate Research and Scholarship Program (UGRASP) at Southern Utah University for helping fund this project. We would also like to recognize and thank Dr. Johnny MacLean and Dr. Fred Lohrengel for helpful revisions, David Maxwell GIS/GPS lab director and specialist at Southern Utah University for useful advice concerning GIS software and data, Dr. Minghua Ren for assistance with electron microprobe analysis, and The University of Nevada Las Vegas Department of Geoscience for allowing the use of the Electron Microanalysis and Imaging Laboratory.

REFERENCES CITED:

Bennett, V.C. and DePaolo, D.J., 1987. Proterozoic crustal history of the western United States as determined by neodymium isotopic mapping. *Geological Society of America Bulletin,* v. 99, p. 674-685.

Colberg, M.R.,2009. The Beaver Dam-Gold Butte trend, Utah and Nevada: a collisonal boundary offering insights into the nature of Yavapai Province crust. *Geological Society of America Abstracts w/Programs,* v. 41, p. 271.

Colberg, M.R., 2011. New constraints of the Paleo-Proterozoic assembly of the southwestern margin of Laurentia: high (ultra-high?) pressure metamorphism in the Mojave-Yavapai suture, Utah, Nevada, Arizona. *Geological Society of America Abstracts w/Programs,* v. 43, p. 3322.

Duebendorfer, E.M., Chamberlain, K.R., and Fry, B., 2006. Majave-Yavapai boundary zone, southwestern United States: a rifting model for the formation of an isotropically mixed crustal boundary zone. *Geology*, v. 34, p. 681-684.

Ernst, W.G. and Liu, J., 1998. Experimental phase-equilibirum study of Al-and T-contents of calcic amphibole in MORB-A semi-quantitative thermo-barometer. *American Mineralogist*, v. 83, p. 952-969.

Faryad, S.W., Dolejs, D., and Machek, M., 2009. Garnet exsolution in pyroxene from clinopyroxenites in the Moldanubian zone: constraining the early pre-convergence history of ultramafic rocks in the Variscan orogeny. *Journal of Metamorphic Geology,* v. 27, p. 655-671.

Fitzgerald, N.E. and Colberg, M.R., 2008. Evidence of Paleo-Proterozoic high-pressure metamorphism and decompression melting in the Majave-Yavapai suture zone, Beaver Dam Mountains, Utah. *Geological Society of America Abstracts w/Programs*, v. 40, p. 64.

GNU, 2012. Veusz General Public License, 1.15.

Green, T.H. and Hellman, P.L., 1982. Fe-Mg partitioning between co-existing garnet and phengite at high pressure, and comments on a garnet-phengite geothermometer. *Lithos*, v. 15, p. 253-256.

Henry, D.J., Guidotti, C.V., and Thomason, J.A., 2005. The Ti-saturation surface for low-to-medium pressure metapelitic biotites: implications for geothermometry and Ti-substitution mechanisms. *American Mineralogist,* v. 90, p. 316-328.

Holland, T. and Blundy, J., 1994. Non-ideal interactions in calcic amphiboles and their bearing on amphibole-plagioclase thermometry. *Contributions to Mineralogy and Petrology,* v. 116, p. 433-447.

Koziol, A.M. and Newton, R.C., 1988. Redtermination of the anorthite breakdown reaction and improvement of the plagioclase-garnet-Al_2SiO_5-quartz barometer. *American Mineralogist*, v. 73, p. 216-223.

Leake, B.E., Wooley, A.R., Arps, C.E.S., Birch, W.D., Gilbert, C.M., Grice, J.D., Hawthorne, F.C., Kato, A., Kisch, H.J., Krivovichev, V.G., Linthout, K., Laird, J., Mandarino, J.A., Maresch, W.V., Nickel, E.H., Rock, N.M.S., Schumacher, J.C., Smith, D.C., Stephenson, N.C.N., Ungaretti, L., Whittaker, E.J.W., and Youzhi, G., 1997. Nomenclature of amphiboles: report of the subcommittee on amphiboles of the International Mineralogical Association, Commission on New Minerals and Mineral Names. *The Canadian Mineralogist*, v. 35, p. 219-246.

Nelson, S.T., Hart, G.L., and Frost, C.D., 2011. A reassessment of Majavia and new Cheyenne Belt of alignment in the eastern Great Basin. *Geosphere*, v. 7, p. 513-527.

Passchier, C.W. and Trouw, R.A.J., 2005. *Microtectonics* (2nd edition), Berlin, Springer, 366 p.

Quigley, M.C., Karlstrom, K.E., Beard, S., and Bohannon, B., 2002. Influence of Proterozoic and Laramide structures on the Miocene extensional strain field, North Virgin Mountains, Nevada/Arizona. *U.S. Geological Survey Open-File Report 02-172*, p. 85-104.

Spear, F.S., 1993. *Metamorphic Phase Equilibria and Pressure-Temperature-Time Paths.* Mineralogical Society of America, 799 p.

Williams, M.L. and Grambling, J.A., 1990. Manganese, ferric iron, and the equilibrium between garnet and biotite. *American Mineralogist*, v. 75, p. 886-908.

Wooden, J.L. and DeWitt, E., 1991. Pb isotopic evidence for a major early crutal boundary in western Arizona, *in*, Karlstrom, K.E., ed., *Proterozoic Geology and Ore Deposits of Arizona*, *Arizona Geological Digest*, v. 19, p. 27-50.

Zhang, R.Y. and Liou, J.G., 1999. Exsolution lamellae in minerals from ultra-high pressure rocks. *International Geology Review*, v. 41, p. 981-993.